Colloid Polym Sci 278:280–284 (2000)

SHORT COMMUNICATION

F. Katzenberg
R. Janlewing
J. Petermann

Surface diffusion of metal atoms on polymer substrates during physical vapour deposition

Received: 9 April 1999
Accepted in revised form: 21 October 1999

F. Katzenberg · R. Janlewing
J. Petermann (✉)
Lehrstuhl für Werkstoffkunde
Fachbereich Chemietechnik
Universität Dortmund
Email–Figge-Strasse 66
D-44227 Dortmund, Germany
e-mail: petermann@chemietechnik.uni-dortmund.de
Tel.: +49-231-7552479
Fax: +49-231-7552480

Abstract The surface diffusion of physical-vapour-deposited metal atoms on thermoplastic polymer substrates was investigated. In accordance with the hypothesis of the "classical" atomistic diffusion model, diffusion coefficients are derived from a Monte Carlo simulation. Because the "classical" atomistic diffusion model neglects the desorption of the metal atoms, the absolute diffusion data obtained in our investigations should only be considered as rough estimates. It is more the intention of our work to present relative values in order to correlate the metal surface diffusion on polymer substrates with their physical states (morphologies and surface dynamics). As expected, the diffusivity of metal atoms is strongly influenced by the chemical affinity ("reactivity") between the metal atoms and the polymer substrate. Furthermore, the diffusivity strongly depends on the physical state of the polymer substrate. On polymer surfaces above the glass-transition temperature the surface diffusivity of metal atoms is 1 order of magnitude higher than the diffusivity below the glass-transition temperature.

Key words Surface diffusion · Metal · Polymer · Microstructure · Monte Carlo

Introduction

There is growing interest in metallized polymers. The spectrum of applications ranges from reflectors to compact discs to electrical shielding/adsorption to thin-film transistors and precision optics [1, 2].

Usually, the polymer substrates are metallized by physical vapour deposition (PVD). Because surface diffusion is one of the basic physical and microstructure-forming processes in PVD metallization, knowledge of the diffusion behaviour and the possibility to control it are very important for microstructural applications. Because in situ observations of the surface diffusion of metal atoms or small clusters on polymer surfaces are difficult, conclusions about the diffusivity were drawn from the cluster sizes and densities with the help of a Monte Carlo simulation. In order to obtain diffusion coefficients from our experimental data, some assumptions regarding condensation coefficients [3] and cluster formations [4] have to be made, which may be considerably reflected in the absolute data. Nevertheless, it is the intention of our work to present and to compare surface diffusion data for different physical states of the polymer surfaces (crystallinity, morphology, etc.).

Experimental

Polymer substrate preparation and metallization

Uniaxially oriented semicrystalline polymer substrates were prepared according to the method of Petermann and Gohil [5]. The commercial polymer granulate was dissolved in 0.5 wt% xylene at a temperature of 423 K. Some droplets of this solution were put on a preheated glass slide with a temperature well above the crystallization temperature of the polymer. The solution was dispersed uniformly and the solvent was allowed to evaporate. From the remaining polymer melt a highly oriented ultrathin polymer film was drawn using a motor-driven cylinder. The thin films were cut into squares, mounted onto conventional transmis-

sion electron microscope (TEM) copper grids and used without further treatment for metallization (PVD) and subsequent TEM investigations. The substrates were vapour-deposited with the respective metals in a Balzers BAE080T evaporation chamber at a pressure of 5×10^{-3} Pa. The nominal layer thickness as well as the deposition rate were monitored with a quartz crystal oscillating microbalance. The subsequent TEM examinations were carried out in a Philips CM200 TEM operating at 200 kV. The polymers used in the present study were high-density and low-density polyethylene (HDPE, Lupolen 6021D and LDPE, Lupolen 1810H) and isotactic polypropylene (iPP, Novolene 1100H) all from BASF (Ludwigshafen, Germany).

Monte Carlo simulation

Because in situ observations of the surface diffusion of metal atoms on polymer surfaces are difficult to perform, conclusions about the diffusivity were made from the microstructure of the resulting metallization layer by comparison of the respective cluster sizes and densities from the experiments with the results of a Monte Carlo simulation.

The simulation is based on the "classical" atomistic diffusion model [6], which assumes only monomer diffusion, stable dimers and statistical nucleation. Desorption and diffusion of adsorbate atoms or adsorbate clusters into the polymer (volume diffusion) are neglected because comparison of the material deposited onto the polymer surface and of that deposited onto the microbalance revealed no differences. Furthermore, no material was discovered underneath the surface in TEM cross-sectional investigations [7]. The hypothesis of statistical nucleation is justified by the statistical cluster distribution of the adsorbate/substrate system examined as well as by the nonappearance of graphoepitaxy or decoration of clusters along surface topologies. Considering the evaporation parameters, such as evaporation rate, nominal layer thickness (from the microbalance) and evaporation time of the real evaporation experiment, the surface diffusion coefficient ($D = 1/4 \times l^2/\tau$) of the vapour-deposited metals on the polymer substrates is derived by the variation of the "hopping frequency", τ^{-1}, and the average "hopping distance", l, of the metal atoms. In the simulation only single atoms perform continuous jumps with random directions (random walk). The polymer surface is modelled as an isotropic continuum. The only obstacles for the random walk are the atoms themselves. Randomly formed dimers or clusters of several atoms are stable and immobile; therefore, clusters are only able to grow and ripening processes are neglected.

These assumptions form a contrast to the effective processes at real polymer surfaces; however, the periodical structure of the crystalline surface areas of the polymer is considered by using typical lattice dimensions for the hopping distances. All the diffusion coefficients were derived by using a hopping distance of 0.6 nm [8, 9], which is equivalent to a typical van der Waals distance.

To get reliable diffusion coefficients, a comparison is necessary between many experiments and the respective Monte Carlo simulations with different evaporation parameters but under equal diffusion conditions because different evaporation rates and nominal layer thicknesses have to result in the same diffusion coefficient on the same polymer substrate at the same substrate temperature. Because coalescence or other ripening processes may influence strongly the evaluation of the cluster sizes and densities and therefore may lead to incorrect diffusion coefficients, all the evaporation experiments were stopped below a layer thickness above which these processes become likely. To minimize the number of evaporation experiments, the polymer surface was shadowed over an obstacle. Because of the non-point-like extensions of the evaporation source, analogous to light optics, a half shadow occurs. The continuum of evaporation rates between the boundaries "directly evaporated – half shadow" and "half shadow – total shadow" was used for the Monte Carlo simulation (Fig. 1). The TEM bright-field micrograph (Fig. 2) shows the half shadow of gold onto HDPE. The dotted line indicates the boundary between the directly evaporated surface area and the half shadow.

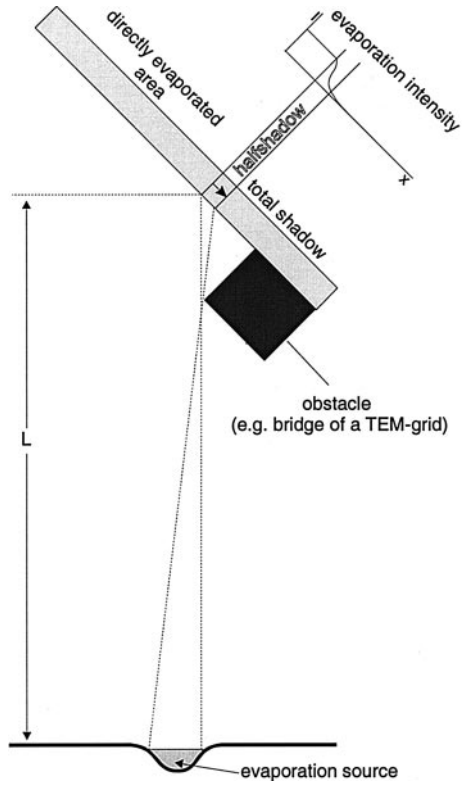

Fig. 1 Sketch to elucidate the origin of the half shadow

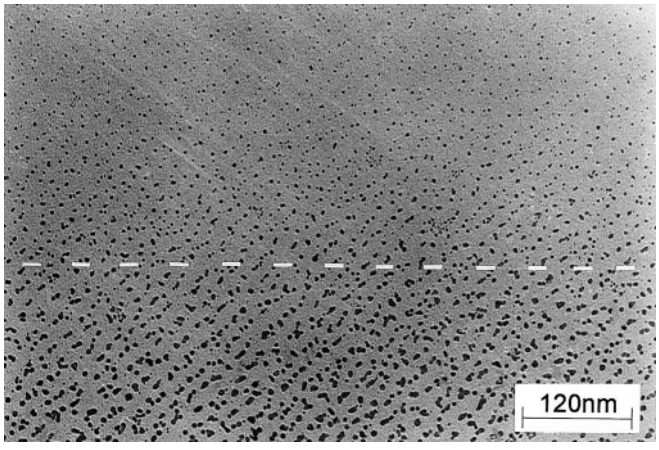

Fig. 2 Transmission electron microscope (*TEM*) bright-field micrograph of gold clusters on an uniaxially oriented high-density polyethylene substrate evaporated with 0.48-nm radiation at an angle of 45° over a bridge of the TEM grid. The *dotted line* shows the boundary between the directly evaporated surface area and the half shadow

Results

For the investigations of the diffusivity of different adsorbates on a polymer surface at room temperature, uniaxially oriented HDPE was used because it cross-links during electron radiation and the resulting radiation resistance [10–12] simplifies the evaluation of the metal clusters in the TEM.

The diffusion coefficients of gold, silver, tin, tellurium and platinum calculated using the Monte Carlo simulation are listed in Table 1. Starting with low values, platinum has the lowest diffusivity of 5×10^{-11} cm^2/s, followed by gold and silver with 4.0×10^{-8} and 9.5×10^{-8} cm^2/s, respectively. Tin and tellurium (1.0×10^{-7} cm^2/s) have a diffusivity twice has high as the other metals.

Gold was used to investigate the diffusivity of an adsorbate on different polymer substrates at room temperature because of its good contrast in the TEM. The surface diffusion coefficients of gold on different polymer substrates are listed in Table 2. The gold atoms exhibit the lowest diffusivity on electron-beam-irradiated HDPE (irradiation dose about 400 C/m^2) of 1.0×10^{-10} cm^2/s followed by that on amorphous carbon of 8.0×10^{-10} cm^2/s. The diffusivity of gold on HDPE of 9.5×10^{-8} cm^2/s does not differ significantly from that on iPP.

For the investigation of the influence of the substrate temperature and the physical state below and above the glass-transition temperature, T_g, on the diffusivity of evaporated metal atoms, iPP was used as the substrate. The dependences of the diffusion coefficients of gold on iPP on the substrate temperature are listed in Table 3. The drastic change in the gold diffusivity in the temperature range between 263 and 283 K is remarkable.

The Arrhenius plot (Fig. 3) shows the logarithm of the diffusion coefficients versus the respective reciprocal substrate temperatures. Above 283 K the gold surface diffusion on iPP shows Arrhenius behaviour with a weak temperature dependence which corresponds to an activation energy for surface diffusion of about 2.14 kJ/mol (0.022 eV) and a frequency factor of 9.6×10^{-8} cm^2/s. Below 263 K the diffusivity also follows Arrhenius behaviour, but with a stronger temperature dependence which corresponds to an activation energy of about 12.1 kJ/mol (0.13 eV) and a frequency factor of 2.2×10^{-7} cm^2/s.

Table 1 Surface diffusion coefficients of different adsorbates on high-density polyethylene (*HDPE*) at room temperature

Deposit	Evaporation rate (nm/min)	Layer thickness (nm)	D_{eff} (293 K) (cm^2/s)
Pt	0.74	0.56	$5 \times 10^{-11} \pm 1 \times 10^{-11}$
Au	0.92	0.84	$4.0 \times 10^{-8} \pm 5 \times 10^{-9}$
Ag	0.72	0.66	$9.5 \times 10^{-8} \pm 5 \times 10^{-9}$
Sn	1.05	0.96	$1.0 \times 10^{-7} \pm 5 \times 10^{-8}$
Te	0.13	0.85	$1.0 \times 10^{-7} \pm 5 \times 10^{-8}$

Table 2 Surface diffusion coefficients of gold on HDPE, low-density polyethylene (*LDPE*), isotactic polypropylene (*iPP*), amorphous carbon and irradiated HDPE at room temperature

Substrate	Evaporation rate (nm/min)	Layer thickness (nm)	D_{eff} (293 K) (cm^2/s)
HDPE	0.92	0.84	$4.0 \times 10^{-8} \pm 5 \times 10^{-9}$
LDPE	0.78	0.71	$9.5 \times 10^{-8} \pm 5 \times 10^{-9}$
iPP	0.99	0.99	$4.0 \times 10^{-8} \pm 5 \times 10^{-9}$
Amorphous carbon	2.05	1.44	$1.0 \times 10^{-8} \pm 5 \times 10^{-9}$
HDPE (irradiated)	0.16	0.40	$8.0 \times 10^{-10} \pm 5 \times 10^{-11}$

Discussion

From our results it can be concluded that the surface diffusivity of different metals on numerous polymer

Table 3 Surface diffusion coefficients of gold on iPP at different substrate temperatures

Temperature (K)	D_{eff}(T) (cm^2/s)
213	$2.5 \times 10^{-10} \pm 5 \times 10^{-11}$
232	$4.1 \times 10^{-10} \pm 5 \times 10^{-11}$
253	$9.0 \times 10^{-10} \pm 5 \times 10^{-11}$
263	$1.3 \times 10^{-9} \pm 5 \times 10^{-10}$
273	$1.0 \times 10^{-8} \pm 5 \times 10^{-9}$
283	$3.5 \times 10^{-8} \pm 5 \times 10^{-9}$
293	$4.0 \times 10^{-8} \pm 5 \times 10^{-9}$
313	$4.3 \times 10^{-8} \pm 5 \times 10^{-9}$
333	$4.5 \times 10^{-8} \pm 5 \times 10^{-9}$
353	$4.7 \times 10^{-8} \pm 5 \times 10^{-9}$
373	$4.9 \times 10^{-8} \pm 5 \times 10^{-9}$
393	$5.0 \times 10^{-8} \pm 5 \times 10^{-9}$

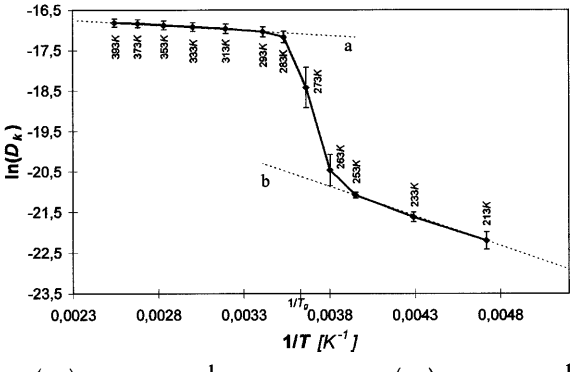

a): $\ln(D_{eff}) = -16{,}2 - 256{,}9 \cdot \frac{1}{T}$ (4.2) b): $\ln(D_{eff}) = -15{,}3 - 1456{,}0 \cdot \frac{1}{T}$ (4.3)

Fig. 3 Arrhenius plot of the temperature dependence of the surface diffusion of gold on isotactic polypropylene

substrates depends on the chemical affinity (reactivity) between adsorbate and substrate. Furthermore, the diffusivity is strongly influenced by the physical state of the substrate (crystalline, amorphous, above/below T_g, etc.).

A reactive metal, such as platinum [13–15], exhibits the lowest diffusivity on semicrystalline polymer surfaces. A microstructure consisting of small and numerous clusters and a closed metallization layer at relatively low nominal layer thicknesses occurs. In contrast, metals such as gold, silver, tellurium or tin [16–18], which show only weak reactivity with the polymeric substrates, exhibit an order of magnitude higher diffusivity on semicrystalline polymer surfaces and a microstructure of relatively big but few clusters.

On comparing the diffusion coefficients of gold on different substrates at room temperature, a lower diffusivity of the gold on HDPE than on LDPE is observed; however, gold has nearly the same surface mobility on iPP and HDPE. Because LDPE and HDPE have the same constitution but differ essentially in their crystallinity, the assumption seems likely that the diffusion coefficient depends on the crystallinity of the polymer substrate. The surface dynamics of the amorphous and crystalline surface areas clearly differs when the polymer is above its T_g (−163 K for HDPE, 273 K for iPP). We use surface dynamics as a synonym for vibration modes, amplitudes and frequencies of the macromolecules in the surface. On comparing the three substrates (iPP, HDPE, LDPE) at room temperature, all three are well above their T_gs, but with HDPE and iPP having about the same crystallinity and LDPE having the highest fraction of the amorphous phase. Above the T_g, the amorphous areas have meltlike behaviour and therefore have higher surface dynamics than the crystalline areas.

According to this assumption, the higher diffusivity of gold on LDPE than on HDPE as well as the comparable diffusivities of gold on HDPE and iPP can be explained by the higher crystallinities of HDPE and iPP than that of LDPE.

This assumption is supported by the diffusion behaviour of gold on iPP at substrate temperatures above and below its T_g, which shows the drastic change of more than 1 order of magnitude in the vicinity of T_g. Because the crystalline parts of the polymer are not influenced by T_g, only the amorphous parts can be responsible for the increase in the surface diffusivity of gold on iPP above T_g. The higher dynamics above T_g is also reflected in the C_p values of the amorphous parts above and below T_g [19].

In the following, ideas are discussed which may explain the surface diffusion mechanism of evaporated adsorbates on the respective microstructural constituents of a semicrystalline polymer substrate depending on its physical state (above/below T_g).

A crystalline surface has periodically arranged surface potentials, also for polymer crystals (Fig. 4, left). Below T_g, surfaces of the amorphous polymer phase have a structure like frozen melts and no periodic arrangements of the atoms or molecules; however, on average, the distances between the molecules and the depth of the potentials do not differ significantly from those of the crystalline surfaces. Consequently, similar surface diffusivities of host atoms (not differing by orders of magnitude) are expected (Fig. 4, right). Because of the higher surface dynamics (conformational changes, motion of entire chain segments, etc.) of the amorphous phase above T_g, additional activation mechanisms for surface diffusion of evaporated adsorbate atoms are likely. The macromolecules permanently change their relative positions to each other. The locally fluctuating average distance, $\overline{r^2}$, of the chains and chain

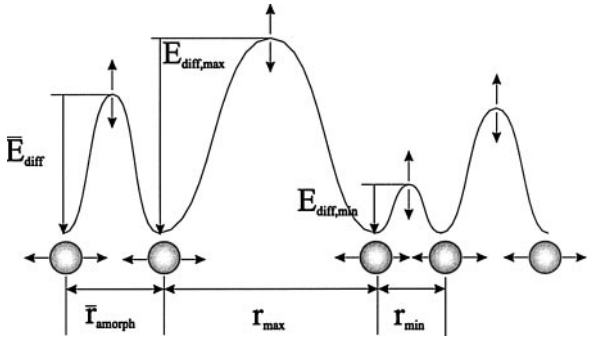

Fig. 5 Fluctuating surface potentials on amorphous polymer surfaces above the glass-transition temperature

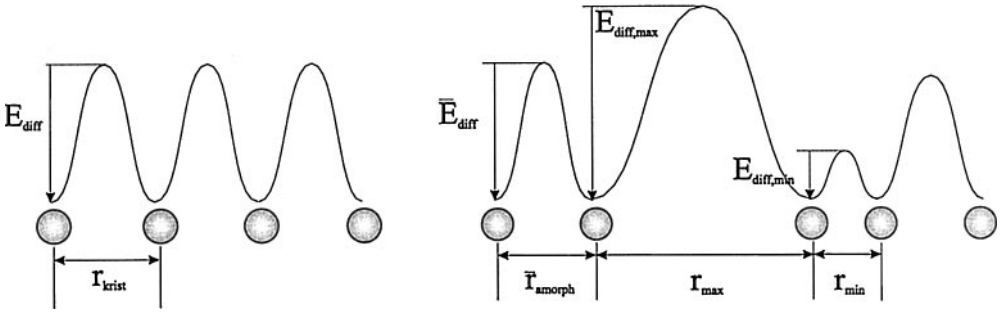

Fig. 4 Surface potentials on crystalline (*left*) and amorphous (*right*) polymer surfaces below the glass-transition temperature

segments results in temporally variable depths and widths of the surface potentials (Fig. 5). Because the depth of the surface potentials or the activation energy, E_{diff}, influences the surface diffusivity exponentially [$D = D_0 \exp(E_{diff}/R\,T)$], such surface dynamics may result in an increase in the hopping probability and consequently in a higher diffusivity of the evaporated adsorbates on amorphous polymer surfaces above T_g.

With this, the activation energy $E_{diff,b}$ for surface diffusivity below T_g is reflected by the average depth of the surface potentials of both the coexisting amorphous and crystalline phases.

Due to the substantially higher value of the activation energy $E_{diff,b}$ (12.1 kJ/mol) of gold surface diffusion on iPP surfaces below T_g than that above T_g ($E_{diff,a}$ = 2.14 kJ/mol) it can be concluded that the surface diffusion above T_g occurs mostly on the amorphous phase.

Accordingly, the metallization of the polymer can be influenced by previous amorphization of the polymer substrate (e.g. by electron-beam irradiation [20]). On the artificially amorphized surface areas, the adsorbate atoms have a clearly different diffusivity that influences the resulting microstructure of the metallization in the course of PVD [20].

Acknowledgement The financial support of the Volkswagen Foundation is gratefully acknowledged.

References

1. Tumula RR, Pamaszewski PJ (1989) Microelectronics packaging handbook. Van Nostrand Reinhold, New York
2. Grebel H, Iskandar B, Pien P, Sheppard K (1990) Appl Phys Lett 57:2959
3. Thran A, Kiene M, Zaporojtchenko V, Faupel F (1999) Phys Rev Lett 82:1903
4. Venables JA (1994) Surf Sci 299:798
5. Petermann J, Gohil RM (1979) J Mater Sci 14:2260
6. Schmidt AA, Eggers H (1996) Surf Sci 349:301
7. Faupel F, et al (1998) In: Mittal Festschrift on Adhesion Science and Technology, van Ooij WJ and Anderson HR Jr. (eds.) VSP, Utrecht, The Netherlands, p. 747–761
8. Katzenberg F (1998) Metallisierung von Polymeren, Reihe 5, Nr. 537. VDI, Dusseldorf
9. Jandt KD, Buhk M, Petermann J, Eng L, Fuchs H (1991) Polym Bull 27:101
10. Dole M (1963) The radiation chemistry of macromolecules, vols 1 + 2. Academic, New York
11. Charlesby A (1986) In: Getoff N (ed) Topics in radiation physics and chemistry. Pergamon, New York, p 134
12. Grubb DT (1974) J Mater Sci 9:1715
13. DiNardo NJ (1989) In: Mittal KL, Susko JR (ed) Metallized plastics 1: fundamentals and applied aspects. Plenum, New York, pp 137–170
14. Bodö P, Sundgren JE (1988) J Vac Sci Technol A 6:2396
15. Freilich SC, Farnsworth FS (1987) Polymer 28:1912
16. Meyer HM, Anderson SG, Atanasoska LJ, Weaver JH (1988) J Vac Sci Technol A 6, 30–37
17. DiNardo NJ, Demuth JE, Clarke TC (1985) Chem Phys Lett 121:239
18. Strunskus T, Grunze M, Kochendoerfer G, Woell Ch (1996) Langmuir 12:2712
19. Wunderlich B (1997) In: Tu EA (ed) Thermal characterization of polymeric materials, vol 1. Academic, New York, p 32
20. Lieberwirth I, Katzenberg F, Petermann J (1998) Adv Mater 10:99